

# TO THE QUESTION OF VERIFICATION OF COLLINEAR CLUSTER TRI-PARTITION (CCT)

Yu.V. Pyatkov<sup>1,2</sup>, D.V. Kamanin<sup>2</sup>, A.A. Alexandrov<sup>2</sup>, I.A. Alexandrova<sup>2</sup>,  
Z.I. Goryainova<sup>2</sup>, V. Malaza<sup>3</sup>, E.A. Kuznetsova<sup>2</sup>, A.O. Strekalovsky<sup>2</sup>,  
O.V. Strekalovsky<sup>2</sup>, V.E. Zhuchko<sup>2</sup>

<sup>1</sup>*National Nuclear Research University MEPhI (Moscow Engineering Physics Institute),  
Moscow, Russia*

<sup>2</sup>*Joint Institute for Nuclear Research, Dubna, Russia*

<sup>3</sup>*University of Stellenbosch, Faculty of Military Science, Military Academy, Saldanha 7395,  
South Africa*

## INTRODUCTION

In recent publications [1–3], we have presented experimental indications of existence of a new at least ternary decay channel of low excited heavy nuclei known as collinear cluster tri-partition (CCT). A fragment mass  $M$  is calculated by the energy  $E$  and the velocity  $V$ . Mainly a scattering of fragments at the entrance of an E-detector gives background events simulating ternary decay. Selection of the “true” events was provided by applying the gates on the fragments momenta, velocities, experimental neutron multiplicity, and the parameters sensitive to the fragment nuclear charge. Observation of the specific linear structures in the  $M_1$ – $M_2$  distributions (mass correlation plots) served as a criterion for a sufficient suppression of the background. The structures were reproduced at the spectrometers of two types. Earlier experiments were performed using gas filled detectors (modules of the FOBOS setup [4]). Later we switched to solid-state detectors, namely timing detectors, on the microchannel plates and the mosaics of PIN diodes (COMETA setup [2] and the similar ones [3]). Even though mass reconstruction procedures for these two types of spectrometers strongly differ, the obtained results are in good agreement.

Estimation of the expected parameters of the CCT products was performed in the recent theoretical works [5–7]. The results obtained were taken into account in our model of the most populated CCT mode known as “Ni-bump”.

## EXPERIMENTS AND RESULTS

Figure 1(a) shows the region of the mass distribution measured at the COMETA setup [2] in the experiment Ex1 for the fission fragments (FFs) from  $^{252}\text{Cf}$  (sf) around the Ni-bump ( $M_1 = 68$ – $80$  amu,  $M_2 = 128$ – $150$  amu). The structures are seen in the spectrometer arm facing the source backing only. No additional selection of the fission events was applied in this case, which resulted in the experiment having almost no background. A rectangular-like structure below the locus of binary fission is bound by magic nuclei (their masses are marked by the numbered arrows), namely  $^{128}\text{Sn}$  (1),  $^{68}\text{Ni}$  (2), and  $^{72}\text{Ni}$  (3). In Figure 1(b), we demonstrate the projection of the linear structure seen at the masses of 68 and 72 amu.

Similar structures were revealed as well in the experiment Ex2 performed at the COMETA-F spectrometer which differs substantially from this used in Ex1 by the data acquisition system based on the fast flash-ADC (CAEN DT5742) and data processing [8].

Due to the background conditions only events with the velocities  $V_2 < 0.8$  cm/ns are presented in Figure 1(c, d). Such selection conditions the difference in the structures below the line  $M_2=68$  amu in the Figure 1(c) comparing Figure 1(a).

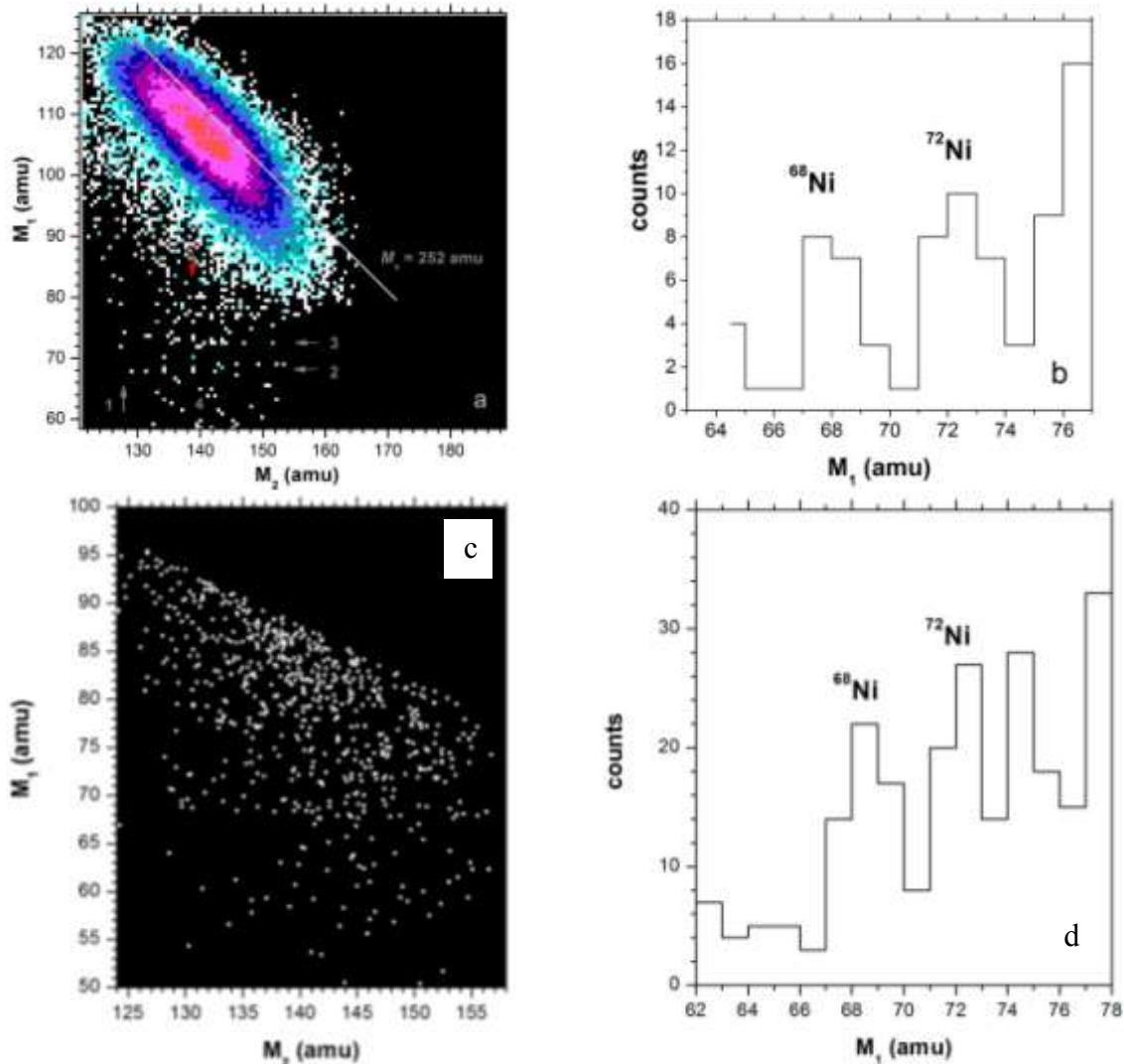


**FIGURE 1.** Region of the mass–mass distribution for the FFs from  $^{252}\text{Cf}$  (sf) around the Ni-bump a) – in Ex1, c) – in Ex2). Projection of the lines 1, 2 onto  $M_1$  axis in Ex1 (b) and in Ex2 (d). It should be indicated that Figures 1(a), (b) were published in Ref. [2].

In fact, only two fragments were detected in each decay event. The mass and velocity of the “missed” fragment could be calculated based on the laws of mass and momentum conservation. In each event showing the missing mass (ternary event), we mark the masses of the fragments in order of their decreasing masses  $M_H$ ,  $M_L$  and  $M_T$  (Ternary particle) respectively. Figure 2(a) demonstrates a correlation between the velocities of two lighter partners of the ternary decay. Only the events for which  $M_L = (67-75)$  amu (Ni-peaks in Figure 1(b)) are under analysis. Their total yield does not exceed  $2.5 \times 10^{-4}$  per binary fission. Three different groups of events are vividly seen in the Figure 1. They are marked by the signs  $w1-w3$  respectively. Each of the loci consists of two subgroups as can be inferred from the plot  $E_L-E_H$  (Figure 2(d)).

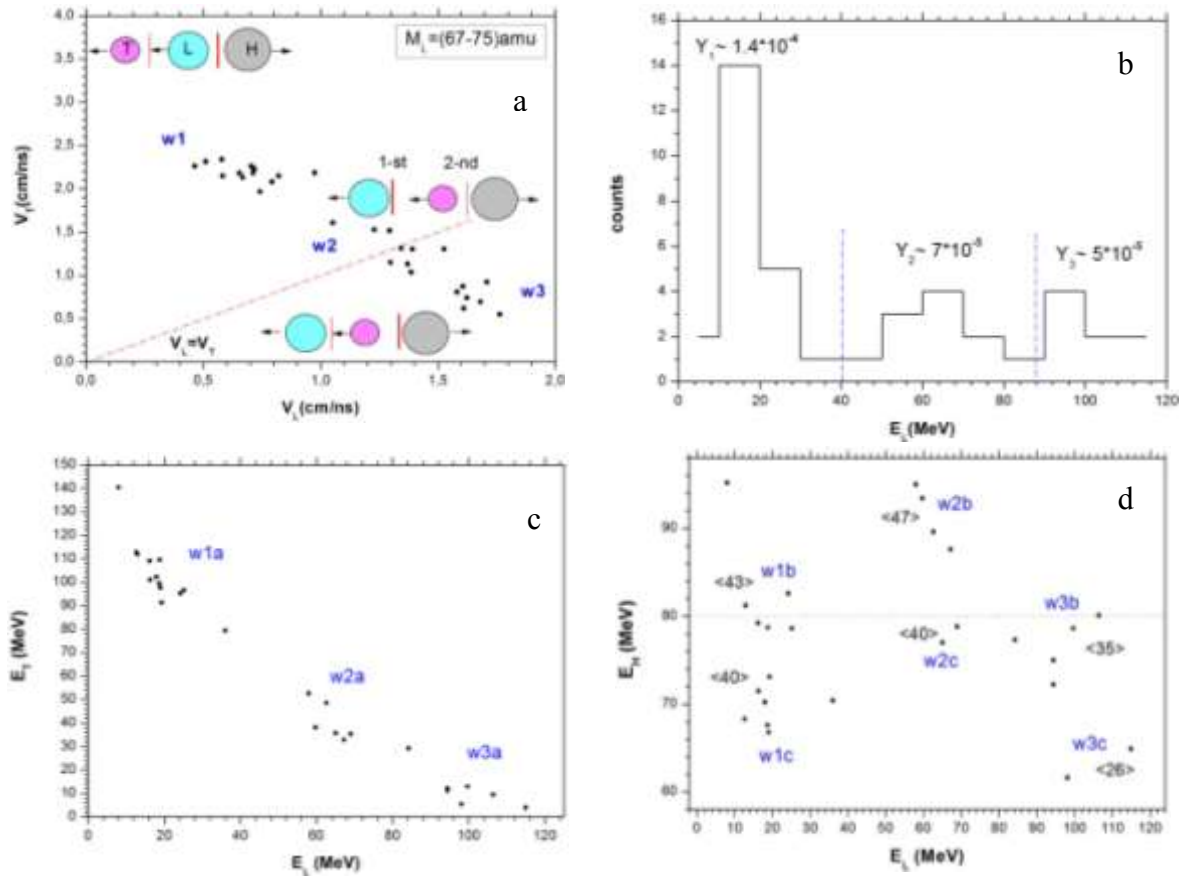


**FIGURE 2.** Ex1: velocities  $V$  and energies  $E$  for the ternary events with  $M_L = (67-75)$  amu (Ni-peaks in Figure 1 (b)). Correlation between the velocities of two lighter partners of the ternary decay – (a), energy spectrum of the detected Ni nuclei (the yields per binary fission are marked above each peak) – (b), energy correlations  $E_L-E_T$  and  $E_L-E_H$  – (c) and (d) respectively. The sketches in the panels illustrate the decay scenario to be discussed below. See the text for details.

## SCISSION POINT CALCULATIONS

Among all the theoretical articles initiated by the results of the experiments, article [6] deserves special attention. Under the three-center shell model the potential energy surfaces for few ternary combinations in a fission channel were calculated for the  $^{252}\text{Cf}$  nucleus. The fission barrier for the  $^{132}\text{Sn} + ^{48}\text{Ca} + ^{72}\text{Ni}$  ternary splitting is shown in Figure 3(a). According to the Figure 3, the exit point corresponds to  $R \sim 22.4$  fm, i.e. elongation of the system exceeds the length of the configuration of three touching spheroids. If just a Ca nucleus took upon itself all extra elongation, the axis ratio of the corresponding spheroid would be approximately 1:1.6.

Calculations [9] performed in ten dimensional deformation space demonstrate the shapes of a decaying Cf nucleus at large deformations (Figure 3(b)) in the potential valleys 3 and 4. The distance between the centers of the side constituents ( $R_{12}$ ) are equal to approximately 18 fm and 23 fm. After the rupture at the narrowest section of the neck, almost all deformation energy concentrates in the light (panel c) or heavy fragment (panel d).

Typical shapes of fissioning nucleus at large deformations are confirmed independently by the neutron data from [10]. For the  $^{248}\text{Cm}$ , such asymmetry in number of emitted neutrons from the light ( $\nu_L$ ) and heavy ( $\nu_H$ ) FFs was traced up to the  $\nu_L/\nu_H = 9/0$ . Just for a sense of the

scale of yields of highly deformed scission configurations, one can cite to the relative total yield  $Y_R$  of the fission events at  $v_{tot} = 6$  and  $v_L/v_H = 6/0$ .  $Y_R$  was estimated to be 2.19 % and 0.72 % for  $^{248}\text{Cm}$  and  $^{252}\text{Cf}$  respectively [11].

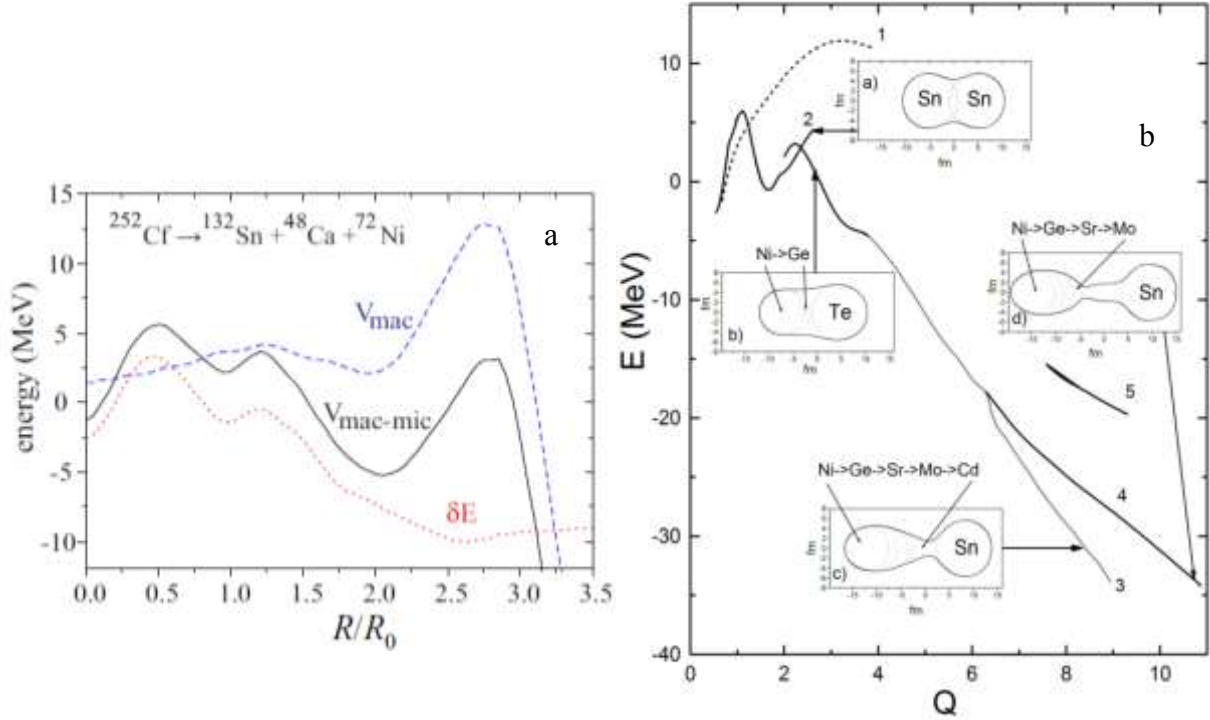


**FIGURE 3.** a) – macroscopic potential energy (dashed line), shell correction (dotted line), and total macro-microscopic potential energy (solid line) of the  $^{252}\text{Cf}$  nucleus corresponding to the  $^{132}\text{Sn} + ^{48}\text{Ca} + ^{72}\text{Ni}$  ternary splitting [6]. Here  $R$  is an approximate distance between the mass centers of the side fragments,  $R_0 = 1.16 A^{1/3}$  is a radius of a mother nucleus; b) – potential energy of a fissioning  $^{252}\text{Cf}$  nucleus, corresponding to the bottoms of the potential valleys, as a function of  $Q$ , proportional to its quadrupole moment. The valleys found are marked by numbers 1 to 5. The panels depict the shapes of the system at the points marked by arrows [9].

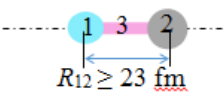
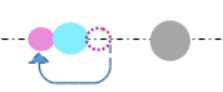
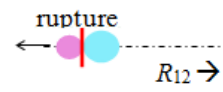
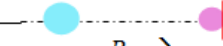
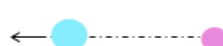
The following scenario of the CCT process can be proposed based on our experimental findings and theoretical calculations. According to Ref. [6], the exit point from under the barrier in the potential valley leading to the  $^{132}\text{Sn} + ^{48}\text{Ca} + ^{72}\text{Ni}$  ternary splitting (Figure 3(a)) corresponds to a much more elongated configuration in comparison with the chain of three touching spherical nuclei. The distance  $R_{12}$  between the centers of the side clusters was estimated to be above  $\sim 23$  fm. Likely, the central fragment (Ca) takes upon itself almost all extra elongation. After a rupture occurs, for instance on the boundary of Ca and Sn clusters, the Ni cluster very quickly (in comparison to full acceleration time) attracts the Ca “neck”. Part of the released deformation energy is spent on emission of neutrons flying apart isotropically. Thus, the formed pear-shaped Ni-Ca dinuclear system can rotate around the center of its gravity by  $180^\circ$ . Such orientation is the most energetically favorable. Octupole vibrations could be another reason for the change in the orientation of the “tip”. Formation of the Ca-Sn system with similar features is less probable [5]. The formed dinuclear system can evolve towards fusion or rupture. In the first case, we deal with a binary fission of a mother nucleus, and in the second instance with a ternary fission.

Presumable decay scenarios for all subgroups are presented in Table I. A precision configuration of the system is demonstrated in the third column of the table. For all the cases fission fragment  $\text{FF}_1$  is supposed to be  $^{70}\text{Ni}$ , the mass of the  $\text{FF}_2$  corresponds to the mean mass

of the lightest cluster (shown in brackets in Figure 3(d)), and the mass of the heavy cluster is calculated using the law of mass conservation. The FFs charges are calculated according to the hypothesis of unchanged charge density. Configurations of the system after the first and the second ruptures are shown respectively in the fourth and the fifth columns of the table.

In the frame of the proposed scenario we have succeeded to reproduce the experimental energies of all three partners of ternary decay (Figure 2). More details results are presented in [12].

**TABLE I.** Pictograms illustrate scenarios of different CCT modes observed in the experiment. See the text for details.

row №	Label of the locus in Fig. 3(d)	Precision configuration of the system	System configuration after the first rupture	System configuration at the moment of the second rupture
1	w1b w1c			
2	w2b w2c	— “ —		
3	w3b w3c	— “ —		
4	binary fission	— “ —		

## CONCLUSIONS

We assume that in contrast to conventional ternary fission the CCT occurs as a two-step decay of an extremely deformed precission nuclear configuration in the valley of true ternary fission [6] or states associated with cold deformed fission in the binary channel [9]. According to the neutron data, the population of such CCT door-states reaches several percent.

As was mentioned above the “Ni-bump” is one of the most populated CCT modes observed and just low energy peak for Ni fragments from the bump (Figure 2(b)) has the greatest yield. Scission point calculations sheds light to the origin of this peak. Summing up, we would recommend registration of the Ni isotopes with the energy lower than 25 MeV at the mass-separator Lohengrin as the primary experiment for independent verification of the CCT.

## ACKNOWLEDGMENTS

This work was supported, in part, by the Russian Science Foundation and fulfilled in the framework of MEPhI Academic Excellence Project (contract 02.a03.21.0005, 27.08.2013) by the Department of Science and Technology of the Republic of South Africa (RSA).

## REFERENCES

1. Yu.V. Pyatkov et al., Eur. Phys. J. A**45**, 29 (2010).
2. Yu.V. Pyatkov et al., Eur. Phys. J. A**48**, 94 (2012).

3. D.V. Kamanin, Yu.V. Pyatkov, Clusters in Nuclei Lecture Notes in Physics 875 vol. 3 ed. C. Beck, Springer, 2013, p. 183.
4. H.-G. Oertlepp et al., Nucl. Inst. Meth A**403**, 65 (1998).
5. A.K. Nasirov, R.B. Tashkhodjaev and W. von Oertzen, Eur. Phys. J. A**52**, 135 (2016).
6. A.B. Karpov, Phys. Rev. C**94**, 064615 (2016).
7. P. Holmval, U. Köster, A. Heinz, and T. Nilsson, Phys. Rev. C**95**, 014602 (2017).
8. Yu.V. Pyatkov et al., J. Phys.: Conf. Series 675, 042018 (2016).
9. Yu.V. Pyatkov et al., Nucl. Phys. A**624**, 140 (1997).
10. V.A. Kalinin et al. in Proc. of the “Seminar on Fission Pont D’Oye V”, Belgium, 2003. World Scientific, Singapore, 2004. p. 73.
11. A.S. Vorobiev, Ph.D. thesis, B. P. Konstantinov Petersburg Institute of Nuclear Physics, 2004 (in Russian, <http://www.gigabaza.ru/doc/2737-all.html>).
12. Yu.V. Pyatkov et al., Phys. Rev. C (2017) (in press).